

Effect of nucleoside analogue antimetabolites on the structure of PEO-PPO-PEO micelles investigated by SANS

Youngkyu Han, Zhe Zhang, Gregory S. Smith, Changwoo Do*

SANS and SAXS analysis for drug-free samples

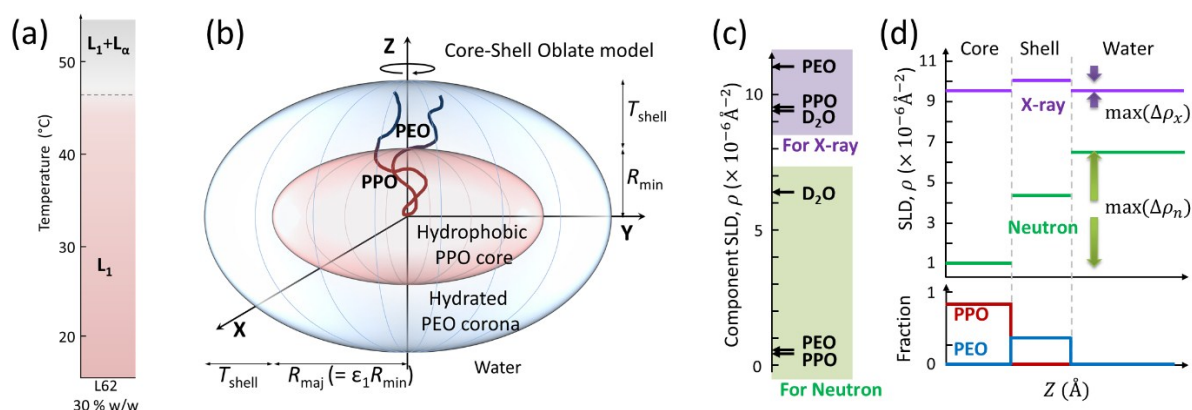


Figure S1. (a) Temperature-dependent Phase behavior of L62 30% w/w aqueous solution in a temperature range between 20°C and 50°C.¹ (b) A schematic diagram of the core-shell oblate model approximately describing the structure of L62 micelles. (c) X-ray and Neutron SLDs of the component molecules, D_2O , PPO, and PEO. (d) An example of molecular distribution of PPO and PEO chains within micelles (bottom) and the corresponding SLD profiles for x-rays and neutrons (top) along the z-axis. The polymer distribution is presumably estimated based on the L62 distribution (Φ_c and Φ_s) at 30°C, which was obtained from SANS analysis. Neutron SLD contrasts in Pluronic micelles are much greater than x-ray SLD contrast.

Pluronic L62 aqueous solution, which is known to exhibit water-rich micellar (L_1), lamellar (L_α), polymer-rich solution (L_2) and multi phases, depending on temperature and concentration, forms a concentrated micellar phase at room temperature at the concentration of 30% w/w (**Figure S1a**). It undergoes a thermodynamic phase transition from the micellar (L_1) phase to the coexistence ($L_1 + L_\alpha$) phase by increasing temperature from 20°C to 50°C. The micellar structure in this temperature range has been investigated using SANS and SAXS experiments. To simultaneously describe the intramicellar structure at 20°C, 30°C, and 40°C, we have used a modified core-shell spheroid form factor in the SANS and SAXS data analysis. Starting from this generalized model, we found that the L62 micelles have an oblate shape consisting of a PPO core, which is characterized by R_{min} and R_{maj} , a PEO shell, which is characterized by T_s , and water layers (**Figure S1b**). Since the neutron and x-ray probes provide totally different scattering length density (SLD) contrasts between the constituent components (**Figure S1c**), the detailed SLD distribution along the radial direction of the core-shell oblates also significantly differ from each other as shown in **Figure S1d**. Our model fitting results indicate that both SANS and SAXS data can be nicely described by the identical model selected, and the good fitting of both data shows that our model is appropriate and our fitting results are reliable. The model fitting results for drug-free samples are summarized in **Table S1** and **S2**.

Table S1. SANS parameters for L62/D2O at 30 % w/w concentration

*Fitted free parameters						
	R_{\min} ($\pm 0.1 \text{ \AA}$)	ε_c (± 0.01)	T_s ($\pm 0.1 \text{ \AA}$)	Φ_c (± 0.01)	φ (± 0.01)	f_{mic} (± 0.01)
20°C	19.7	1.83	7.6	0.48	0.21	0.64
30°C	21.7	1.90	6.4	0.89	0.34	0.73
40°C	22.8	2.03	7.1	0.94	0.31	0.83
50°C	22.8	2.95	8.7	0.89	0.32	0.90
**Secondary parameters calculated using the fitted parameters						
	R_{maj} ($\pm 0.2 \text{ \AA}$)	ε_s (± 0.01)	R_{HS} ($\pm 0.2 \text{ \AA}$)	Core SLD ($\pm 5.0\text{E-}08 \text{ \AA}^2$)	Shell SLD ($\pm 2.0\text{E-}07 \text{ \AA}^2$)	N_{agg} (± 0.3)
20°C	36.1	1.60	43.7	3.47E-06	5.6E-06	16.0
30°C	41.2	1.70	47.6	1.07E-06	4.4E-06	42.3
40°C	46.3	1.79	53.5	0.76E-06	4.3E-06	59.7
50°C	67.1	2.41	75.8	1.03E-06	4.5E-06	118.5

*Data fitted to the core-shell oblate model; R_{\min} , radius of minor axis of core; ε_c , aspect ratio of a core; T_s , thickness of shell; Φ_c , polymer volume fraction in core; φ , effective volume fraction of hard-core interaction radius of micelles; f_{mic} , a fraction of L62 forming micelles. **Secondary parameters obtained from the fitted parameters; R_{maj} , radius of major axis of core; ε_s , aspect ratio of a shell; R_{HS} , effective hard-sphere radius; N_{agg} , aggregation number. The uncertainties of the parameters in the parentheses are the fitting errors from the model fit analysis. These uncertainties are underestimated, because our assumptions make the fitting condition so tight due to the constraints between parameters that the degrees of freedom of the fitting parameters can be remarkably reduced in the multi-dimensional space.

Table S2. SAXS parameters for L62/D2O at 30 % w/w concentration

	*Fixed parameters using SANS results			**Free parameters				
	R_{HS}	T_s	Φ_c	ε_c	φ	A	$q_c (\text{\AA}^{-1})$	$\zeta (\text{\AA})$
20°C	43.7	7.6	0.484	1.8 ± 3.8	0.11 ± 0.34	0.012 ± 0.004	0.11 ± 0.03	28 ± 22
30°C	47.6	6.4	0.887	1.6 ± 0.3	0.26 ± 0.05	0.028 ± 0.006	0.11 ± 0.01	36 ± 12
40°C	53.5	7.1	0.939	1.7 ± 0.2	0.26 ± 0.03	0.042 ± 0.007	0.10 ± 0.01	45 ± 10

*These parameters are fixed at the values obtained from SANS model analysis. **These parameters are set to be free during SAXS fitting; A , the broad peak strength; q_c , the broad peak center corresponding to the length scale of the compositional fluctuation; ζ , the characteristic length of the fluctuation.

Structure factor : random hard-sphere structure factor $S_{HS}(q)$

For the structure factor of the micellar phase, the inter-micellar interaction was assumed to be approximated to the random hard-sphere structure factor²⁻⁴ without solving the Ornstein-Zernicke equation to obtain the complete set of partial structure factors $\{S_{ij}(q)\}$, based on the assumptions that 1) the anisotropy of the spheroid shapes is moderate ($\varepsilon_s < 1.8$ at 20-40°C), 2) the orientations of the spheroids are uncorrelated with position, and 3) the spheroids have unrestricted rotational degrees of freedom at the given concentration

$$S_{mic}(q) = \frac{1}{1 + 24\varphi H(y,\varphi)} \quad (S1)$$

Here $H(y,\varphi)$ is a function of $y(=2qR_{HS})$ and φ , where R_{HS} is the effective hard-sphere radius, and φ is the hard-sphere volume fraction.

$$H(y,\varphi) = \frac{\alpha}{y^3} \{\sin y - y \cos y\} + \frac{\beta}{y^4} \{2y \sin y + (2 - y^2) \cos y\} \quad (S2)$$

, where α , β , and γ are defined by φ ,

$$\alpha = \frac{(1 + 2\varphi)^2}{(1 - \varphi)^4}, \quad \beta = \frac{-6\varphi(1 + 0.5\varphi)^2}{(1 - \varphi)^4}, \quad \gamma = \frac{0.5\varphi(1 + 2\varphi)^2}{(1 - \varphi)^4} \quad (S3)$$

SANS results for drug-loaded samples

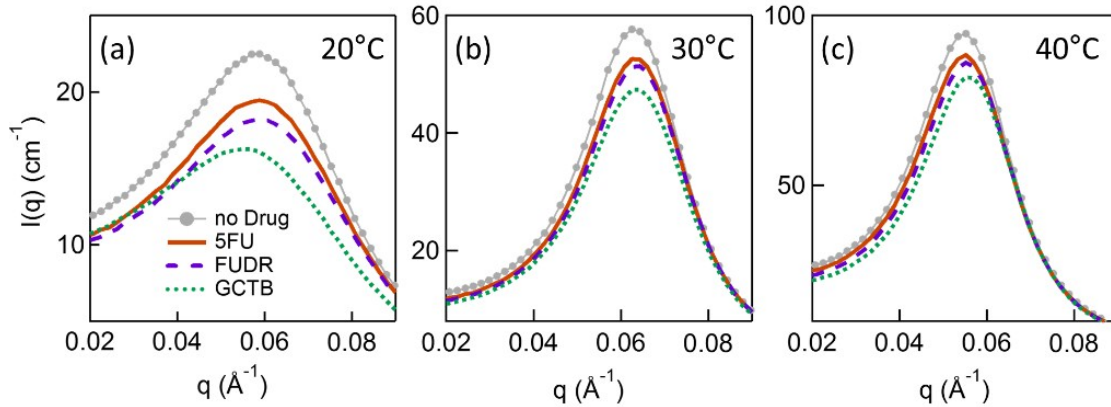


Figure S2. SANS data for the drug-loaded (2%) samples at (a) 20°C, (b) 30°C, and (c) 40°C in linear-linear plot; no drug (closed circle), 5FU (solid), FUDR (dashed), and GCTB (dotted).

Although the drug-induced effects on SANS intensities seem to be insignificant in log-log plot, their effects are distinguishable. The SANS intensity at low-to-intermediate q regions can be reduced about 5-7% by adding 1% w/w drug molecules and about 10-15% by adding 2% w/w. In **Figure S2**, SANS data for the drug-loaded (2% w/w) samples are shown in comparison with the drug-free sample as examples. GCTB affects the intensity most strongly among the selected drugs, followed by FUDR

and 5FU, and this trend has been reflected in the fitting parameters as presented in the manuscript. The SANS fitting results for the drug-loaded samples are summarized in **Table S3**.

Table S3. Results from SANS analysis for the L62/D₂O solution with drug molecules.

Drug	Drug % (w/w)	R_{\min} (± 0.1 Å)	ε_c (± 0.01)	T_s (± 0.1 Å)	Φ_c (± 0.01)	N_{agg} (± 0.3)	Core SLD ($\pm 5.0\text{E-}08$ Å ²)	Shell SLD ($\pm 2.0\text{E-}07$ Å ²)	
20°C	5FU	1	19.3	1.83	7.7	0.45	14.0	3.67 E-06	5.69 E-06
		2	19.3	1.83	7.8	0.44	13.6	3.75 E-06	5.72 E-06
	FUDR	1	19.5	1.82	7.7	0.43	13.6	3.82 E-06	5.72 E-06
		2	19.1	1.83	7.6	0.42	12.5	3.88 E-06	5.74 E-06
	GCTB	1	19.7	1.81	7.8	0.41	13.3	3.92 E-06	5.74 E-06
		2	19.3	1.83	7.6	0.35	11.0	4.25 E-06	5.82 E-06
30°C	5FU	1	21.5	1.90	6.5	0.83	38.2	1.41 E-06	4.58 E-06
		2	21.5	1.90	6.4	0.81	37.1	1.54 E-06	4.62 E-06
	FUDR	1	21.6	1.90	6.4	0.81	37.9	1.54 E-06	4.58 E-06
		2	21.4	1.90	6.4	0.79	35.9	1.66 E-06	4.66 E-06
	GCTB	1	21.5	1.90	6.5	0.80	36.7	1.62 E-06	4.66 E-06
		2	21.3	1.89	6.7	0.74	32.7	1.94 E-06	4.86 E-06
40°C	5FU	1	22.7	2.03	7.1	0.90	56.0	1.02 E-06	4.45 E-06
		2	22.7	2.03	7.2	0.87	54.3	1.16 E-06	4.53 E-06
	FUDR	1	22.8	2.03	7.2	0.87	55.0	1.18 E-06	4.51 E-06
		2	22.8	2.02	7.0	0.86	53.5	1.24 E-06	4.48 E-06
	GCTB	1	22.8	2.03	7.0	0.87	54.8	1.18 E-06	4.48 E-06
		2	22.9	2.00	6.8	0.83	51.3	1.41 E-06	4.50 E-06

Simplified SANS fitting model and its influence at high- q regions

In this work, we have used a modified core-shell spheroid model to describe the micellar structure. The model was simplified, based on two assumptions regarding the radial SLD profile and the size polydispersity of micelles.

Radial SLD profile: The polymeric micelles are usually supposed to have a fuzzy interface between solvent and shell layers, which can be approximated by a decaying function like a parabolic or a cubic function. However, in the form factor of our model, the solid PPO core and PEO/water shell are considered only, and the fuzzy interface is not considered for simplification. We aimed to focus on the drug-induced changes in the averaged properties of a core and a shell in this investigation, assuming that the detailed textures appeared at the high- q region (such as smoothly decaying shell profiles, scattering contributions from polymer blobs) can be ignored.

Polydispersity: It is also unlikely that self-assembled objects such as polymeric micelles are perfectly monodispersed. For polymeric micelles, the aggregation number N is supposed to have a polydispersity to some extent, which may depend on environmental conditions. If we consider core-shell spheres as a model system for micelles, the polydisperse N -distribution will be reflected in the size distribution of spheres. In **Figure S3 (a)**, scattering intensities of core-shell spheres with different core polydispersity $p = 0.05, 0.1, 0.2,$ and 0.3 are presented. They show that a change in core polydispersity affects the intensity level of low- q plateau as well as the oscillation amplitude of intermediate-to-high q transition region. However, as shown in **Figure 1** and **Figure S2**, our SANS data don't show such changes after adding three model drugs. The curve shapes are quite similar in the intermediate and high q regions under the given condition. This implies that addition of the three model drugs doesn't significantly affect the micellar polydispersity, or at least, SANS measurement couldn't capture the changes in the micellar polydispersity. Based on the results that i) the data curves could be nicely fitted using our model without polydispersity and ii) the polydispersity is not the parameter that can be affected by adding drugs, we assumed that the micellar polydispersity doesn't need to be considered in this model analysis to minimize the fitting parameters.

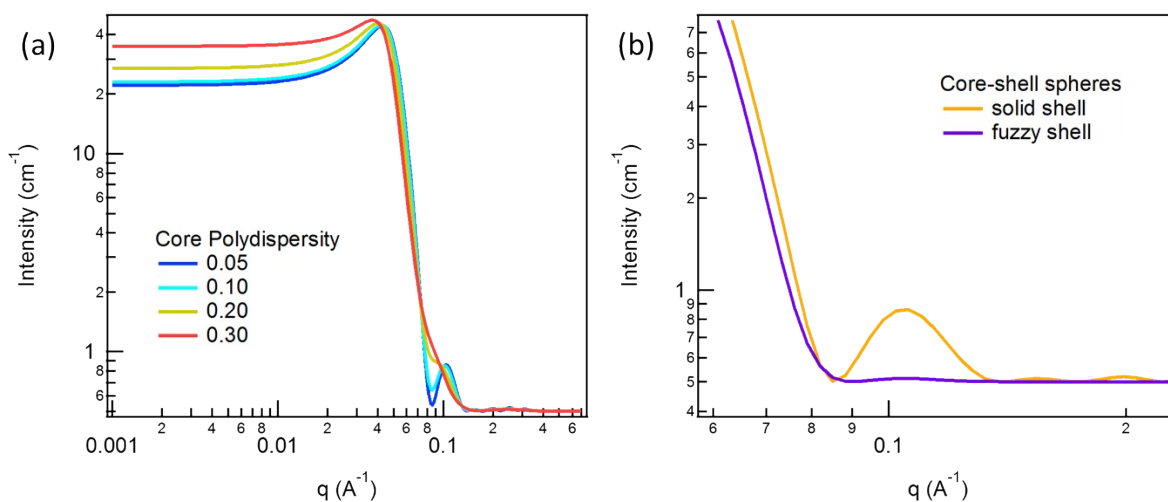


Figure S3. Scattering intensities of core-shell spheres ($R_{\text{core}} = 40 \text{ \AA}$) at volume fraction $\phi = 0.25$; (a) core-shell spheres with different core polydispersity $p = 0.05, 0.1, 0.2, 0.3$ ($p = \sigma/R_{\text{core}}$, where σ^2 is the variance of the distribution of R_{core}) and (b) monodispersed core-shell spheres with a solid shell profile (orange) and a fuzzy shell profile (purple). Incoherent background contribution ($= 0.5 \text{ cm}^{-1}$) is added to the calculated intensities.

As mentioned in the manuscript, the fitting curve can nicely describe the overall shape of the SANS intensities, but the fits are not perfect at the high- q regions. We suppose that the deviations between the SANS data and the fitting curve at $q > 0.1 \text{ \AA}^{-1}$ are attributed to the simplified shell SLD profile as well as the monodispersed core distribution in our model form factor. Our assumptions enhance the form factor oscillation amplitude around the intermediate-high q region; as shown in **Figure S3 (a-b)**, the simplified models with a monodispersed size distribution or a solid shell SLD profile have strong undulations around the region between intermediate and high q . These comparisons can demonstrate that the fitting quality becomes not so good in the q region of $q > 0.1 \text{ \AA}^{-1}$ due to the simplification of the model form factor.

References

1. P. Alexandridis, D. Zhou and A. Khan, *Langmuir*, 1996, **12**, 2690–2700.

2. Ashcroft, N. W. & Lekner, J. Structure and Resistivity of Liquid Metals. *Phys. Rev.* **145**, 83–90 (1966).
3. Kinning, D. J., & Thomas, E. L. Hard-sphere interactions between spherical domains in diblock copolymers. *Macromolecules* **17**, 1712-1718. (1984).
4. Mortensen, K. & Pedersen, J. S. Structural study on the micelle formation of poly(ethylene oxide)-poly(propylene oxide)-poly(ethylene oxide) triblock copolymer in aqueous solution. *Macromolecules* **26**, 805–812 (1993).